

Second Law Analysis of Magneto Radiative GO-MoS₂/H₂O-(CH₂OH)₂ Hybrid Nanofluid

Adnan¹, Umar Khan², Naveed Ahmed³, Syed Tauseef Mohyud-Din⁴, Dumitru Baleanu^{5,6,7},
Kottakkaran Soopy Nisar⁸ and Ilyas Khan^{9,*}

¹Department of Mathematics, Mohi-ud-Din Islamic University, Nerian Sharif AJ&K, 12080, Pakistan

²Department of Mathematics and Statistics, Hazara University, Mansehra, 21120, Pakistan

³Department of Mathematics Faculty of Sciences, HITEC University, Taxila Cantt, 47070, Pakistan

⁴University of Multan, Multan, 66000, Pakistan

⁵Department of Mathematics, Cankaya University, Ankara, Turkey

⁶Institute of Space Sciences, Magurele, 077125, Romania

⁷Department of Medical Research, China Medical University Hospital, China Medical University, Taichung, Taiwan

⁸Department of Mathematics, College of Arts and Sciences, Prince Sattam bin Abdulaziz University,
Wadi, Aldawaser, 11991, Saudi Arabia

⁹Faculty of Mathematics and Statistics, Ton Duc Thang University, Ho Chi Minh City, 72915, Vietnam

*Corresponding Author: Ilyas Khan. Email: ilyaskhan@tdtu.edu.vn

Received: 17 September 2020; Accepted: 12 December 2020

Abstract: Entropy Generation Optimization (EGO) attained huge interest of scientists and researchers due to its numerous applications comprised in mechanical engineering, air conditioners, heat engines, thermal machines, heat exchange, refrigerators, heat pumps and substance mixing etc. Therefore, the study of radiative hybrid nanofluid (GO-MoS₂/C₂H₆O₂-H₂O) and the conventional nanofluid (MoS₂/C₂H₆O₂-H₂O) is conducted in the presence of Lorentz forces. The flow configuration is modeled between the parallel rotating plates in which the lower plate is permeable. The models which govern the flow in rotating system are solved numerically over the domain of interest and furnished the results for the temperature, entropy generation and thermophysical characteristics of the hybrid as well as conventional nanofluids, respectively. It is examined that the thermal profile intensifies against stronger thermal radiations and magnetic field. The surface of the plate is heated due to the imposed thermal radiations and magnetic field which cause the increment in the temperature. It is also observed that the temperature declines against more rotating plates. Further, the entropy production increases for more dissipative effects and declines against more magnetized fluid. Thermal conductivities of the hybrid nanofluid enhances promptly in comparison with regular liquid therefore, under consideration hybrid nanofluid is reliable for the heat transfer. Moreover, dominating thermal transport is perceived for the hybrid nanofluid



This work is licensed under a Creative Commons Attribution 4.0 International License, which permits unrestricted use, distribution, and reproduction in any medium, provided the original work is properly cited.

which showed that hybrid suspension GO-MoS₂/C₂H₆O₂-H₂O is better for industrial, engineering and technological uses.

Keywords: Heat transfer; thermal radiation; Entropy Generation; GO-MoS₂ hybrid nanoparticles; thermophysical characteristics

1 Introduction

The analysis of heat transfer is a topic of interest due to its variety of applications comprised in various industries and engineering. The remarkable applications of thermal transport are comprised in pharmaceutical, microelectronics, fuel cells, heat exchanger, home appliance and domestic refrigerator etc. To finish the production process of many industrial ingredients, a huge amount of heat is required. The conventional liquids like kerosene oil, engine oil, ethylene glycol EG and water are less heat transfer fluids which fail to provide the considerable heat transfer. Therefore, researchers and engineers paved their attentions to overcome these major issues of daily life, industrialist and engineers. They thought that the heat transfer in regular liquids (mentioned above) can be enhanced by adding an extra nanomaterial known as nanoparticles in the host liquid. Finally, a new class of heat transfer fluids was developed and termed as Nanofluid. Nanofluids are colloidal mixture of nanomaterial and host liquid in which both the host fluid and the nanomaterial are thermally in equilibrium. These fluids overcome the issues faced by the engineers and industrialist. Despite that nanofluids have an extra heat transfer characteristics, scientists and engineers thought that a new hybrid class of fluids could be developed and focused on a new type of fluids which has remarkable heat transfer properties as compared to that of regular liquids and nanofluids, respectively. This newly developed class is termed as Hybrid Nanofluid. These fluids are the coupling of hybrid nanoparticles in the base liquid or hybrid base liquid. The development of this newly developed heat transfer fluids almost covers the issues of the industrialist.

Hybrid nanofluids are colloidal suspension of the hybrid nanomaterials into the host liquids. Thermal conductance of the hybrid nanomaterials is high in comparison with conventional nanomaterials. Due to high thermal conductance, hybrid nanofluids are superior over the conventional nanoliquids. Therefore, the hybrid nanoliquids are extensively used in various industries where a large amount of heat transfer is required to accomplish the production processes. The applications of these fluids comprised in medical sciences, chemical engineering, biotechnology, computer chips, coatings, catalytic purposes, civil engineering, flow characteristics of the fluids in various geometries and coatings of the vehicles and in cancer therapy.

Hybrid nanofluids became very popular among the researchers, engineers and industrialist due to their better heat transfer characteristics. Therefore, researchers examined the influences of hybrid nanofluids in the flow regimes, heat transfer rate and local nusselt number in different geometries by considering different flow conditions at the boundaries and far away from the surface. In 2019, Ahmed et al. [1] examined the flow of water suspended by hybrid nanoparticles of Ag-Fe₃O₄ between Riga plates. In order to discuss more physical aspects of the flow regimes, they incorporated the influences of nonlinear thermal radiations and chemical reaction phenomenon in the energy and concentration constitutive relations, respectively. Das et al. [2] considered Cu-Al₂O₃/H₂O hybrid nanofluid in the porous channel. Also, they encountered second law analysis and found the interesting results.

The second law analysis in the hybrid nanofluid composed by graphene and ferromagnetic nanoparticles was presented in [3]. They explored the results for thermal enhancement in the

hybrid nanofluid by incorporating the magnetic field effects in the energy equation. The remarkable influences of magnetic field in the momentum and temperature of the hybrid nanofluid were examined. In 2018, Humnic et al. [4] discussed the heat transfer rate and entropy generation analysis in a flattened tube. To enhance the amount of heat transfer, they used the hybrid nanofluid and found fascinating results for entropy generation and heat transfer characteristics. In 2017, Hussain et al. [5] explored the mixed convection flow by considering the colloidal suspension of the host liquid suspended by the hybrid nanoparticles in a cavity placed horizontally. The fascinating results regarding to entropy generation and influences of magnetic field were discussed in their study. Three-dimensional squeezing flow of the hybrid liquid (water-EG) saturated by hybrid nanoparticles ($\text{Fe}_3\text{O}_4\text{-Ag}$) was presented in [6]. An effective thermal conductivity model based on various shape factors of the hybrid nanoparticles was emerged in the energy equation for better thermal enhancement. A comparative colloidal study of the nanofluid and hybrid nanofluid by considering the forced convection effects was reported in [7]. They treated the models numerically and found the results for the flow regimes and the heat transfer characteristics.

Thermal enhancement and entropy generation inspection between the parallel rotating plates situated in Cartesian frame is a topic of interest due to its multifarious applications in chemical and mechanical industries. In 2017, Ahmed et al. [8] reported the flow of chemically reacting fluid over an unsteady stretchable surface. They incorporated the influences of linear thermal radiations and cross diffusion gradients in the energy and concentration laws. They also examined the effects of convective condition in the heat transfer rate and reported the interesting results. A novel investigation of heat transfer analysis in water and EG saturated by γ -nanoparticles was examined in [9]. The effects of an effective Prandtl number are also embedded in the energy equation that showed an interesting behavior of heat transfer. Khan et al. [10] reported the numerical analysis of the nanofluids containing γ -nanoparticles and reported the fascinating results for the velocity, temperature and heat transfer. Furthermore, useful analysis of the nanofluids by considering the important flow conditions were described in [11,12].

From the literature study, it is noted that entropy generation and temperature investigation in $\text{GO-MoS}_2/\text{C}_2\text{H}_6\text{O}_2\text{-H}_2\text{O}$ hybrid nanofluid between parallel rotating plates is not reported so far. Therefore, this study is makeup to fill this significant research gap. For improved temperature and entropy generation. Moreover, thermal radiations and magnetic field effects are plugged in the energy and momentum relations. The resultant hybrid model is then tackled by numerical scheme known as RK technique. The results for the velocity, temperature and entropy generation are plotted and discussed comprehensively and finally concluding remarks of the analysis are presented.

2 Statement Geometry and Hybrid Model Formulation

2.1 Statement and Geometry

2.1.1 Nanomaterial and Host Liquid

Three-dimensional rotating flow of hybrid nanofluid between the parallel plates is considered in which:

- i. $\text{C}_2\text{H}_6\text{O}_2\text{-H}_2\text{O}$ is taken as hybrid base liquid
- ii. GO-MoS_2 is taken as hybrid nanomaterial.

2.2 Conditions and Assumptions

The following conditions are imposed during the analysis:

- i. The colloidal suspension is viscous.
- ii. The colloidal suspension is an incompressible.
- iii. The hybrid nanoliquid and hybrid nanomaterial are thermally compatible.
- iv. The flow of the hybrid nanofluid is electrically conducting and thermal radiations effects are considered.
- v. The flow is unsteady.
- vi. The lower plate is static at $y = 0$ and upper plate is at height h and is defined as
$$h = \left(\frac{v(1-ct)}{a} \right)^{0.5}.$$
- vii. The squeezed velocity of the hybrid nanofluid is $V_h(t)$.
- viii. The nanofluid and the plates are rotating together oriented counter clockwise with rotating velocity $\Omega = \omega_j(1-ct)^{-1}$.
- ix. The plate at lower end is permeable and sucks the hybrid nanofluid with velocity $-V_0/(1-ct)$.
- x. The lower plate is stretched along x -axis with $U_w = ax(1-ct)^{-1}$.
- xi. Magnetic field is applied perpendicularly with intensity $B_0(1-ct)^{-0.5}$.

The flow model of the hybrid nanofluid is obtained in the view of aforementioned assumptions and the flow configuration is depicted in [Fig. 1](#).

2.3 Governing Hybrid Model

By implementing the above-mentioned assumptions, the following magneto radiative and dissipative hybrid nanofluid model is obtained in dimensional form [13]:

$$\frac{\partial u}{\partial x} + \frac{\partial v}{\partial y} + \frac{\partial w}{\partial z} = 0, \quad (1)$$

$$\Xi_1 \left(\frac{\partial u}{\partial t} + u \frac{\partial u}{\partial x} + v \frac{\partial u}{\partial y} + 2\omega_0(1-ct)^{-1}w \right) = -\frac{\partial p}{\partial x} + \Xi_2 \left(\frac{\partial^2 u}{\partial x^2} + \frac{\partial^2 u}{\partial y^2} \right) - \frac{\Xi_3 B_0^2}{(1-ct)}u, \quad (2)$$

$$\Xi_1 \left(\frac{\partial v}{\partial t} + u \frac{\partial v}{\partial x} + v \frac{\partial v}{\partial y} \right) = -\frac{\partial p}{\partial y} + \Xi_2 \left(\frac{\partial^2 v}{\partial x^2} + \frac{\partial^2 v}{\partial y^2} \right), \quad (3)$$

$$\Xi_1 \left(\frac{\partial w}{\partial t} + u \frac{\partial w}{\partial x} + v \frac{\partial w}{\partial y} - 2w_0(1-ct)^{-1}u \right) = \Xi_2 \left(\frac{\partial^2 w}{\partial x^2} + \frac{\partial^2 w}{\partial y^2} \right) - \frac{\Xi_3 B_0^2}{(1-ct)}w, \quad (4)$$

$$\begin{aligned} \left(\frac{\partial T}{\partial t} + u \frac{\partial T}{\partial x} + v \frac{\partial T}{\partial y} \right) &= \frac{\Xi_4}{\Xi_5} \left(\frac{\partial^2 T}{\partial x^2} + \frac{\partial^2 T}{\partial y^2} \right) + \frac{16\sigma^* T_\infty^3}{3k^* \Xi_5} \frac{\partial^2 T}{\partial y^2} + \Xi_2 \left(4 \left(\frac{\partial u}{\partial x} \right)^2 \right. \\ &\quad \left. + \left(\frac{\partial u}{\partial y} + \frac{\partial v}{\partial x} \right)^2 + \left(\frac{\partial w}{\partial x} \right)^2 \left(\frac{\partial w}{\partial y} \right)^2 \right), \end{aligned} \quad (5)$$

here, Ξ_i for $i = 1, 2, \dots, 5$, represents an effective density, dynamic viscosity, electrical conductivity, thermal conductivity and heat capacity, respectively. The effective models for the conventional and hybrid nanofluids are as follows [14].

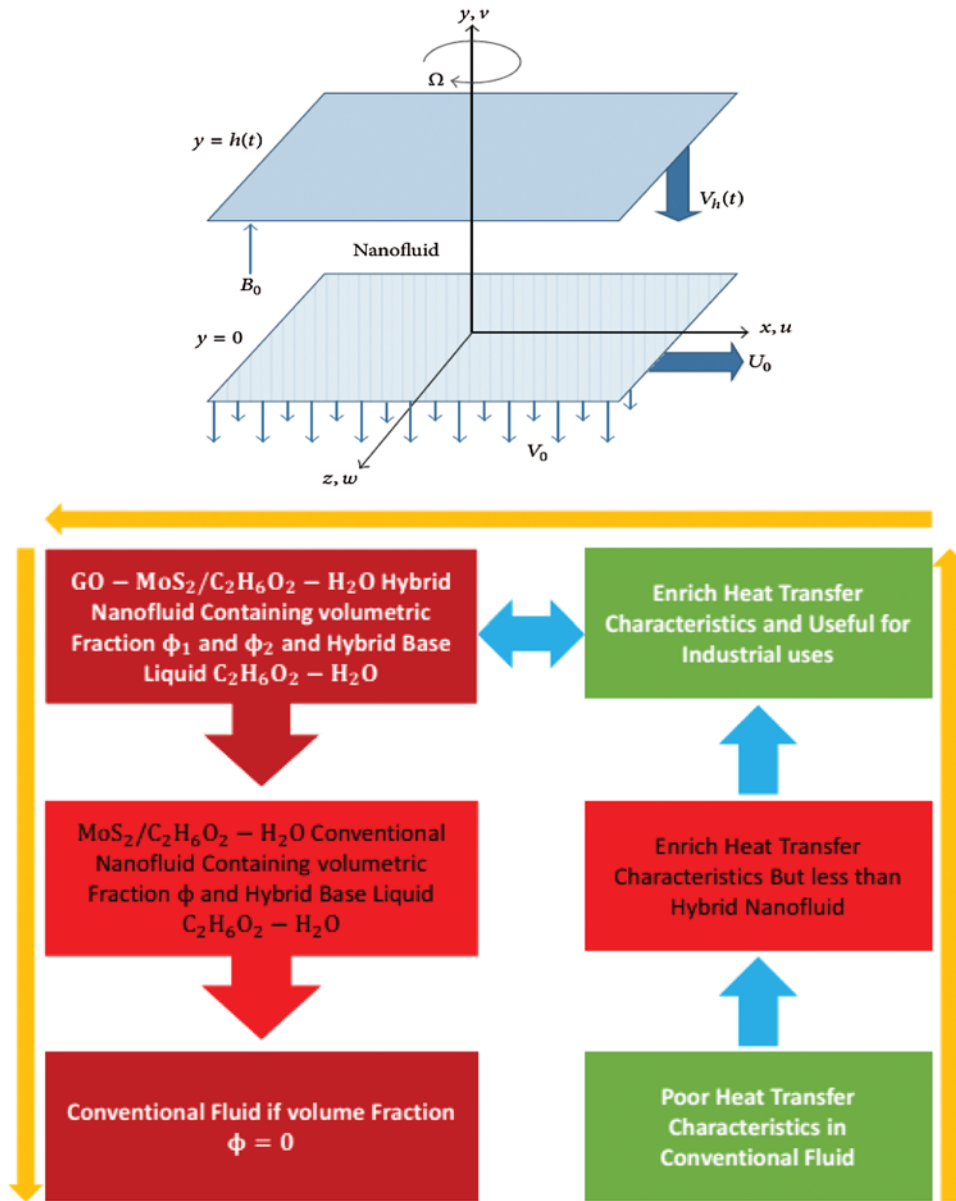


Figure 1: Configuration of the hybrid nanofluid GO-MoS₂/C₂H₆O₂-H₂O flow

In [Tab. 1](#), m is the shapes factor and different values of m lead to three different types of nanomaterial. The shapes of these nanoparticles are given in [Tab. 2](#).

Thermophysical properties of under consideration hybrid liquid (H₂O-C₂H₆O₂) and hybrid nanoparticles (GO-MoS₂) are described in [Tab. 3](#).

Table 1: Effective models for the conventional and hybrid nanofluids

Ξ_i	Properties	GO/C ₂ H ₆ O ₂ -H ₂ O conventional nanofluid	GO-MoS ₂ /C ₂ H ₆ O ₂ -H ₂ O hybrid nanofluid
Ξ_1	Density	$\frac{\rho_{nf}}{(1-\phi)+\phi\frac{\rho_s}{\rho_f}} = \rho_f$	$\frac{\rho_{hnf}}{(1-\phi_2)\left((1-\phi_1)+\phi_1\frac{\rho_{s1}}{\rho_f}\right)+\phi_2\rho_{s2}} = \rho_f$
Ξ_2	Dynamic viscosity	$\mu_{nf}(1-\phi)^{2.5} = \mu_f$	$\mu_{hnf}(1-\phi_1)^{2.5}(1-\phi_2)^{2.5} = \mu_f$
Ξ_3	Electrical conductivity	$\frac{\sigma_{nf}}{\left(1+\frac{\left(\frac{\sigma_s}{\sigma_f}-1\right)\phi}{\left(\frac{\sigma_s}{\sigma_f}+2\right)-\left(\frac{\sigma_s}{\sigma_f}-1\right)\phi}\right)} = \sigma_f$	$\frac{\sigma_{hnf}}{\left(1+\frac{3\phi\left(\phi_1\sigma_1+\phi_2\sigma_2-\sigma_{bf}\left(\phi_1+\phi_2\right)\right)}{\left(\phi_1\sigma_1+\phi_2\sigma_2+2\phi\sigma_{bf}\right)-\sigma_{bf}\phi\left(\phi_1\sigma_1+\phi_2\sigma_2\right)-\sigma_{bf}\left(\phi_1+\phi_2\right)}\right)} = \sigma_{bf}$
Ξ_4	Thermal conductivity	$\frac{k_{nf}}{\left(\frac{k_s+(m-1)k_f-(m-1)(k_f-k_s)\phi}{k_s+(m-1)k_f+(k_f-k_s)\phi}\right)} = k_f$	$\frac{k_{hnf}}{\left(\frac{k_{s2}+(m-1)k_{bf}-(m-1)(k_{bf}-k_{s2})\phi_2}{k_{s2}+k_{bf}(m-1)+(k_{bf}-k_{s2})\phi_2}\right)} = k_{bf}$ and $\frac{k_{bf}}{\left(\frac{k_{s1}+(m-1)k_f-(m-1)(k_f-k_{s1})\phi_1}{k_{s1}+(m-1)k_f+(k_f-k_{s1})\phi_1}\right)} = k_f$
Ξ_5	Heat capacity	$\frac{(\rho c_p)_{nf}}{\left(1-\phi+\frac{\phi(\rho c_p)_s}{(\rho c_p)_f}\right)} = (\rho c_p)_f$	$\frac{(\rho c_p)_{hnf}}{\left(1-\phi_2\left((1-\phi_1)+\phi_1\frac{(\rho c_p)_{s1}}{(\rho c_p)_f}\right)+\phi_2(\rho c_p)_{s2}\right)} = (\rho c_p)_s$
Ξ_6	Thermal expansion coefficient	$\frac{(\rho\beta)_{nf}}{\left(1-\phi+\frac{\phi(\rho\beta)_s}{(\rho\beta)_f}\right)} = (\rho\beta)_f$	$\frac{(\rho\beta)_{hnf}}{\left(1-\phi_2\left((1-\phi_1)+\phi_1\frac{(\rho\beta)_{s1}}{(\rho\beta)_f}\right)+\phi_2(\rho\beta)_{s2}\right)}$

Table 2: Shape Factor for three different sort of nanoparticles


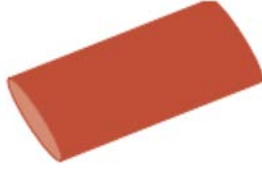
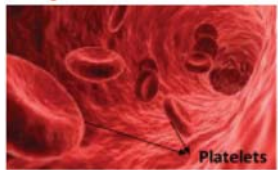
Bricks	Cylinders	Platelets
		
Shape Factor for Bricks Sphericity:3.7	Shape Factor for Cylinders Sphericity:4.9	Shape Factor for Platelets Sphericity:5.7

Table 3: Thermophysical attributes of the hybrid liquid and hybrid nanoparticles

Thermophysical characteristics	Unit	Hybrid host liquid	Nanoparticles	
		C ₂ H ₆ O ₂ -H ₂ O	MoS ₂	GO
ρ	kg/m^3	1063.8	5060	1800
c_p	J/kgK	3630	397.21	717
k	W/mK	0.387	904.4	5000
β^*	$1/K$	5.8×10^{-4}	2.8424×10^{-5}	2.84×10^{-4}
σ	$1/\Omega m$	9.75×10^{-4}	2.09×10^4	6.30×10^7

The flow conditions at the plates are defined as:

$$\left. \begin{aligned} u &= U_w = ax(1-ct)^{-1} \\ v &= -V_0(1-ct)^{-1} \\ w &= 0 \\ T &= T_w \end{aligned} \right\} \text{ at } y=0, \text{ (lower permeable plate),} \tag{6}$$

and

$$\left. \begin{aligned} u &= 0 \\ v &= V_h = -\frac{c}{2} \left(\frac{v}{a(1-ct)} \right)^{0.5} \\ w &= 0 \\ T &= T_h \end{aligned} \right\} \text{ at } y=h(t), \text{ (at upper plate)} \tag{7}$$

For the particular hybrid model, the similarity variables are as follows [13]:

$$\left. \begin{aligned} u &= U_w F' \left(\frac{y}{h(t)} \right) \\ v &= \sqrt{\frac{av}{a(1-ct)}} F \left(\frac{y}{h(t)} \right) \\ w &= U_w G \left(\frac{y}{h(t)} \right) \\ \beta \left(\frac{y}{h(t)} \right) &= \frac{T - T_w}{T_w - T_h} \\ \eta &= \frac{y}{h(t)} \end{aligned} \right\} \text{ similarity transformations} \tag{8}$$

Incorporating the feasible invertible transformations and the partial derivatives in the governing equations, the following two models are obtained on the basis of the nanofluid models.

2.4 Dimensionless GO-MoS₂/C₂H₆O₂-H₂O Model

$$\begin{aligned} F'''' - \left((1-\phi_2) \left((1-\phi_1) + \phi_1 \frac{\rho_{s1}}{\rho_f} \right) + \phi_2 \rho_{s2} \right) (1-\phi_1)^{2.5} (1-\phi_2)^{2.5} (3F'F'' - FF''') + \frac{S}{2} (3F'' + \eta F''') + 2\Omega G' \\ - (1-\phi_1)^{2.5} (1-\phi_2)^{2.5} \left(1 + \frac{3\phi(\phi_1\sigma_1 + \phi_2\sigma_2 - \sigma_{bf}(\phi_1 + \phi_2))}{(\phi_1\sigma_1 + \phi_2\sigma_2 + 2\phi\sigma_{bf}) - \sigma_{bf}\phi((\phi_1\sigma_1 + \phi_2\sigma_2) - \sigma_{bf}(\phi_1 + \phi_2))} \right) M^2 F'' = 0, \end{aligned} \tag{9}$$

$$G'' + \left((1-\phi_2) \left((1-\phi_1) + \phi_1 \frac{\rho_{s1}}{\rho_f} \right) + \phi_2 \rho_{s2} \right) (1-\phi_1)^{2.5} (1-\phi_2)^{2.5} (FG' - F'G + 2\Omega F' - S \left(G + \frac{\eta}{2} G' \right)) - (1-\phi_1)^{2.5} (1-\phi_2)^{2.5} \left(1 + \frac{3\phi(\phi_1\sigma_1 + \phi_2\sigma_2 - \sigma_{bf}(\phi_1 + \phi_2))}{(\phi_1\sigma_1 + \phi_2\sigma_2 + 2\phi\sigma_{bf}) - \sigma_{bf}\phi((\phi_1\sigma_1 + \phi_2\sigma_2) - \sigma_{bf}(\phi_1 + \phi_2))} \right) M^2 G = 0 \quad (10)$$

$$\left(1 + \frac{Rd}{\left(\frac{k_{s2} + (m-1)k_{bf} - (m-1)(k_{bf} - k_{s2})\phi_2}{k_{s2} + k_{bf}(m-1) + (k_{bf} - k_{s2})\phi_2} \right)} \right) \beta'' - \frac{\text{Pr} \left((1-\phi_2) \left((1-\phi_1) + \phi_1 \frac{(\rho c_p)_{s1}}{(\rho c_p)_f} \right) + \phi_2 (\rho c_p)_{s2} \right)}{\left(\frac{k_{s2} + (m-1)k_{bf} - (m-1)(k_{bf} - k_{s2})\phi_2}{k_{s2} + k_{bf}(m-1) + (k_{bf} - k_{s2})\phi_2} \right)} \times \left(F\beta' + \frac{S}{2}\eta\beta' \right) = 0. \quad (11)$$

The dimensional flow conditions reduced in the following dimensionless form:

$$\left. \begin{array}{l} F(\eta) = A \\ F'(\eta) = 1 \\ G(\eta) = 0 \\ \beta(\eta) = 1 \end{array} \right\} \text{ at } \eta = 0 \text{ (lower plate).} \quad (12)$$

and

$$\left. \begin{array}{l} F(\eta) = \frac{S}{2} \\ F'(\eta) = 0 \\ G(\eta) = 0 \\ \beta(\eta) = 0 \end{array} \right\} \text{ at } \eta = 1 \text{ (upper plate).} \quad (13)$$

The dimensionless flow parameters embedded in the flow models are defined by the following mathematical formulas:

$$A = \frac{V_0}{ah}, \quad S = \frac{c}{a}, \quad \Omega = \frac{\omega_0}{a}, \quad Pr = \frac{\mu_f (C_p)_f}{k_f}. \quad (14)$$

2.5 Entropy Formulation

The entropy generation for the under-consideration hybrid models are given in the following way [15]:

$$S_{G^*} = \frac{k_f}{T_0^2} \left(\Xi_4 + \frac{16\sigma^* T_h^3}{3k_f K^*} \right) \left(\left(\frac{\partial T}{\partial x} \right)^2 + \left(\frac{\partial T}{\partial y} \right)^2 \right) + \frac{\Xi_2}{T_h} \left(4 \left(\frac{\partial u}{\partial x} \right)^2 + \left(\frac{\partial u}{\partial y} + \frac{\partial v}{\partial x} \right)^2 + \left(\frac{\partial w}{\partial x} \right)^2 + \left(\frac{\partial w}{\partial y} \right)^2 \right) + \frac{\Xi_3 B_0^2}{T_0} u^2$$

$$\text{(Thermal + Radiative irreversibility) + (viscous dissipation irreversibility)} \quad (15)$$

here, Ξ_4 and Ξ_2 are described in [Tab. 1](#) for the conventional and hybrid nanofluids, respectively.

The entropy generation due to radiative heat flux, thermal transport and friction of the hybrid nanoliquid are incorporated in Eq. (15). By plugging the appropriate invertible transformations in Eq. (15) and after performing the mathematical calculation, the following dimensionless expression is attained:

$$N_g = \frac{S_{G^*}}{S_{G_0^*}} \tag{16}$$

$$N_g = (\Xi_4 + \text{Rd}) \beta'^2 + \text{Pr} (\Omega^{-1}) \Xi_2 (Ec (F'^2 + G^2) + E_{cx} (F''^2 + G'^2)) + \Xi_3 MF'^2 \tag{17}$$

In Eq. (17), the characteristics entropy generation is expressed by the following formula:

$$S_{G_0^*} = \frac{k (T_w - T_h)^2}{h^2 T_h^2} \tag{18}$$

The dimensionless thermal difference (Ω) appeared in Eq. (17) is expressed in the following form:

$$\alpha = (T_w - T_h)/T_h \tag{19}$$

By incorporating the expressions of Ξ_4 and Ξ_2 , in Eq. (20), the following mathematical relations are obtained for the hybrid and conventional nanoliquids.

$$N_g = \left(\frac{k_f}{\left(\frac{k_s + (m-1)k_f - (m-1)(k_f - k_s)\phi}{k_s + (m-1)k_f + (k_f - k_s)\phi} \right) + \text{Rd}} \right) \beta'^2 + \frac{\text{Pr} (\alpha^{-1}) (Ec (F'^2 + G^2) + E_{cx} (F''^2 + G'^2))}{(1 - \phi)^{2.5}} + \Xi_3 MF'^2 \tag{20}$$

(MoS₂/C₂H₆O₂-H₂O)

and for hybrid nanoliquid (GO-MoS₂/C₂H₆O₂-H₂O) is expressed as:

$$N_g = \left(k_{bf} \left(\frac{k_{s2} + (m-1)k_{bf} - (m-1)(k_{bf} - k_{s2})\phi_2}{k_{s2} + k_{bf}(m-1) + (k_{bf} - k_{s2})\phi_2} \right) + \text{Rd} \right) \beta'^2 + \frac{\text{Pr} (\alpha^{-1}) (Ec (F'^2 + G^2) + E_{cx} (F''^2 + G'^2))}{(1 - \phi_1)^{2.5} (1 - \phi_2)^{2.5}} + \Xi_3 MF'^2 \tag{21}$$

3 Mathematical Treatment of ZnO-SAE50

Under-consideration models are highly coupled and nonlinear in nature. Therefore, exact solutions for such models are incredible. Thus, the numerical technique together with shooting method is adopted for the solutions purpose [10]. For initiation of the technique, first order IVP is obtained by using the following transformations and obtained the solutions of the models.

$$b_1 = F, \quad b_2 = F', \quad b_3 = F'', \quad b_4 = F''', \quad b_5 = G, \quad b_6 = G', \quad b_7 = \beta, \quad b_8 = \beta'. \tag{22}$$

Fig. 2 represents the solution steps for the implemented mathematical technique. The following flowchart represents the implementation of the technique.

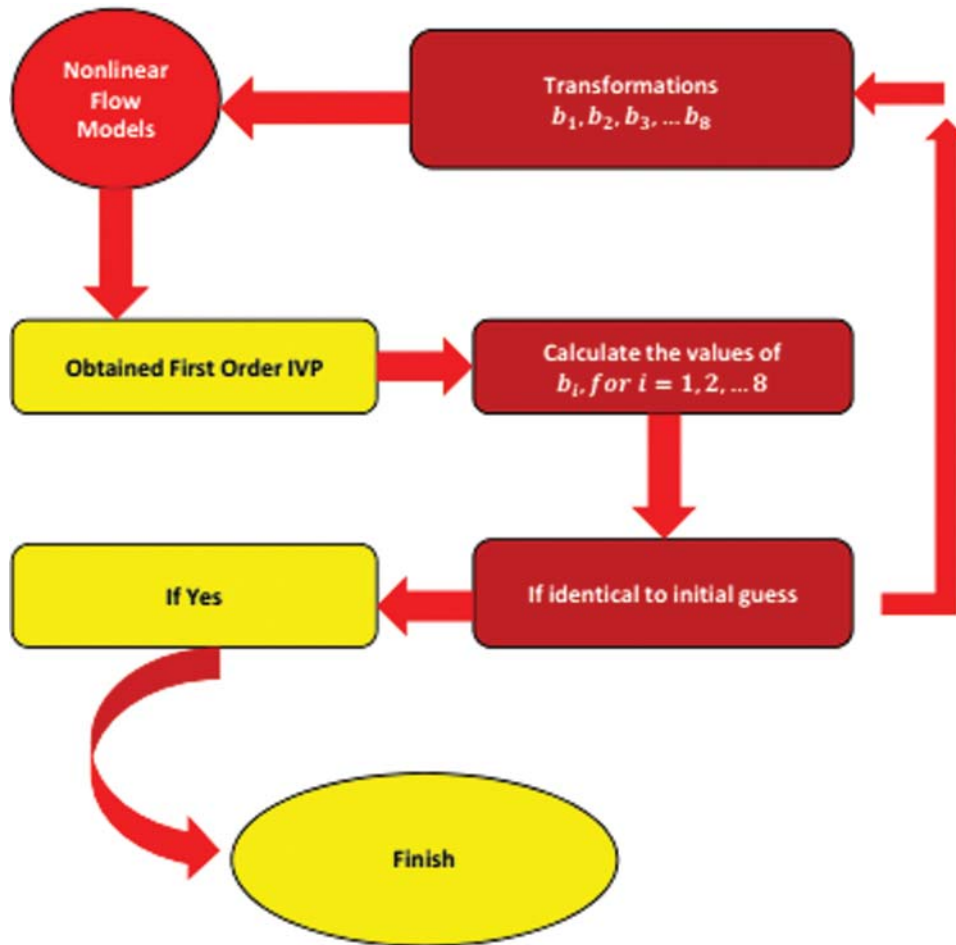


Figure 2: Flow chart for mathematical analysis of the models

4 Discussion of the Results

4.1 Thermal Field

Fig. 3 is plotted to analyze the behavior of GO-MoS₂/C₂H₆O₂-H₂O and MoS₂/C₂H₆O₂-H₂O temperature against varying thermal radiations R_d . It is perceived that the temperature $\beta(\eta)$ enhances against stronger thermal radiations for both nanofluids. Physically, the plates are heated due to thermal radiations effects due to which the internal kinetic energy of the fluid particles increases and consequently the temperature rises. For $S > 0$, thermal field enhances abruptly because the fluid particles compressed together due to the movement of upper plate in the direction of lower once and more energy transferred between the fluid molecules which lead to increment in the fluid temperature. On the other side, slow increment in the thermal field is perceived because the energy transport between the fluid particles become slow due to away movement of the upper plate. Fig. 4 pointed the effects of Ω on the thermal field $\beta(\eta)$. The rotational parameter Ω resists the nanofluids temperature. The decrement in the temperature is examined slow against $S > 0$ in comparison with $S < 0$.

Fig. 5 is decorated to analyze the thermal behavior $\beta(\eta)$ against the induced magnetic field. It is pointed that the stronger magnetic field favors the temperature of GO-MoS₂/C₂H₆O₂-H₂O and

MoS₂/C₂H₆O₂-H₂O nanofluids. For $S > 0$ (upper plate moves in the direction of lower plate), abrupt increment in $\beta(\eta)$ is examined because due to more squeezing effects the temperature rises abruptly. In GO-MoS₂/C₂H₆O₂-H₂O hybrid nanofluid, the temperature enhances due to larger fraction factor. For $S < 0$, the temperature rises slowly. Physically, for $S < 0$, more free area produced between the plates and more particles move to fill the free space and consequently the velocity drops. Due to this decrement in the velocity, the particles friction drops and consequently the temperature rises slowly.

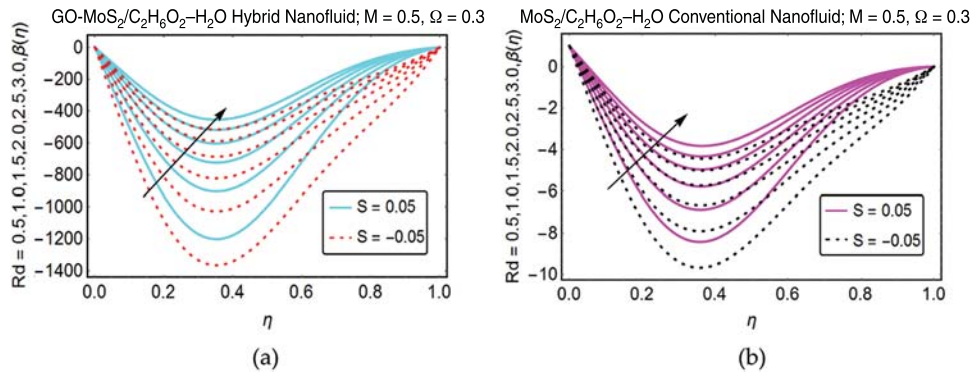


Figure 3: Influence of Rd on (a) hybrid nanofluid (b) conventional nanofluid on $\beta(\eta)$

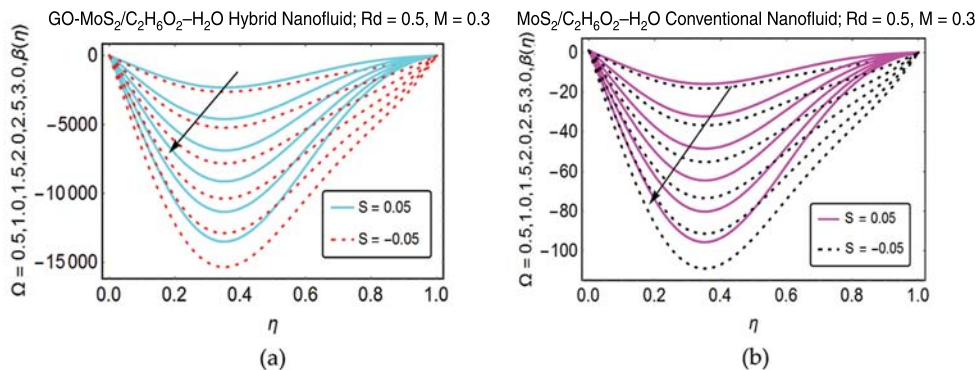


Figure 4: Influence of Ω on (a) hybrid nanofluid (b) conventional nanofluid on $\beta(\eta)$

4.2 Entropy Analysis

The study of second law in magneto radiative nanofluids is a potential topic of interest in fluid dynamics. It is the amount of entropy produced during irreversible process. The applications of this phenomena comprised in heat pumps, air conditioners, refrigerators, heat exchanges, thermal mechanics and mixing or expanding of substances.

The effects of numerous parameters on the entropy generation in GO-MoS₂/C₂H₆O₂-H₂O and MoS₂/C₂H₆O₂-H₂O are pointed in Figs. 6-12. It is perceived that the entropy declines for stronger induction of magnetic field. For GO-MoS₂/C₂H₆O₂-H₂O abrupt decrement is perceived near the lower plate. These effects are decorated in Fig. 6. The rotational parameter Ω resists the entropy for both sort of nanofluids.

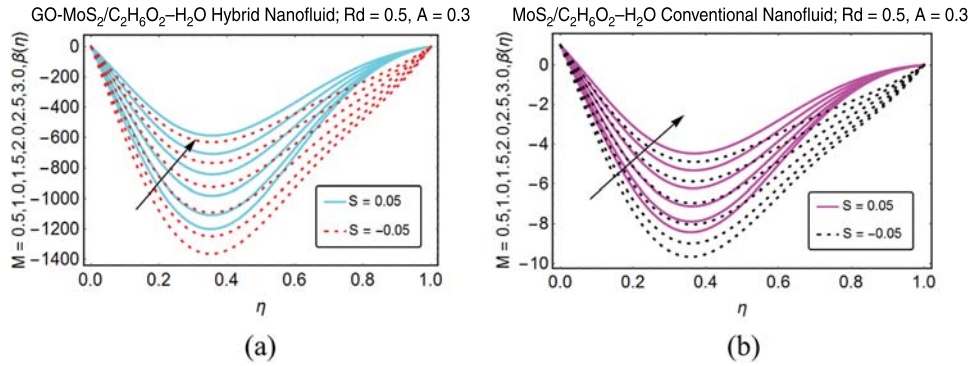


Figure 5: Influence of M on (a) hybrid nanofluid and (b) conventional nanofluid on $\beta(\eta)$

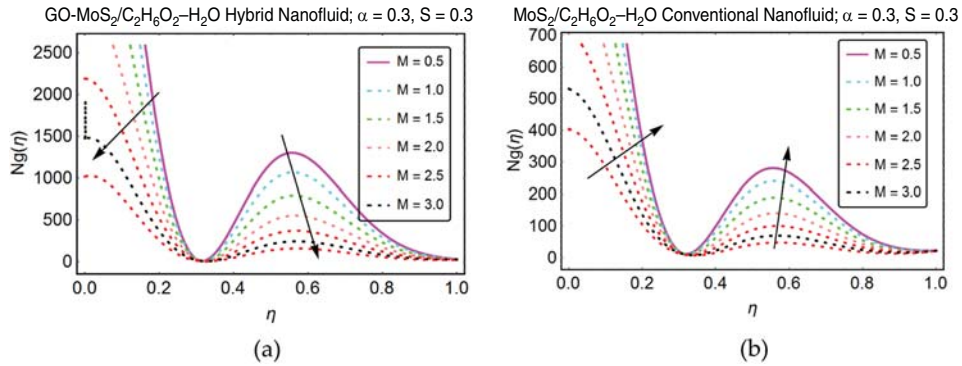


Figure 6: Influence of M on entropy generation for (a) hybrid nanofluid (b) conventional nanofluid

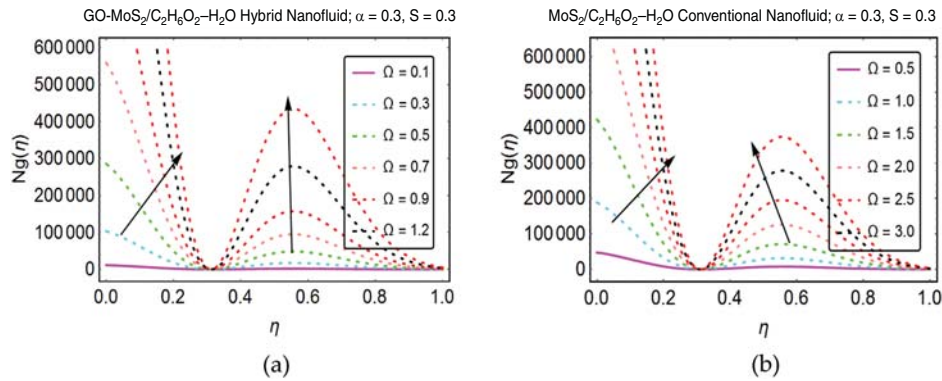


Figure 7: Influence of Ω on entropy generation for (a) hybrid nanofluid (b) conventional nanofluid

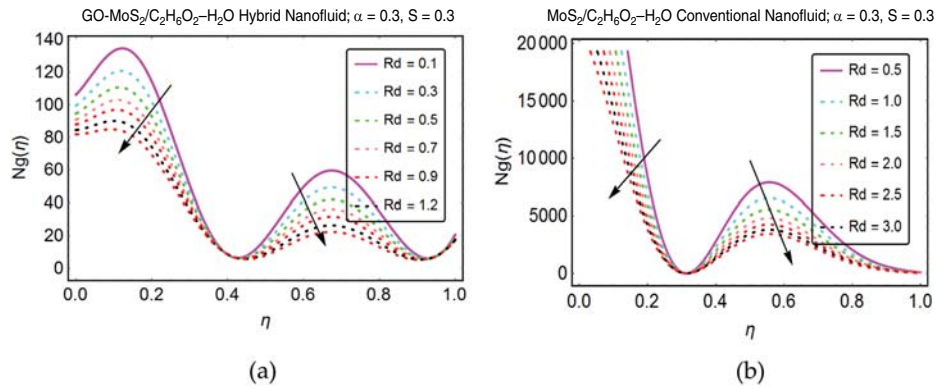


Figure 8: Influence of Rd on entropy generation for (a) hybrid nanofluid and (b) conventional nanofluid

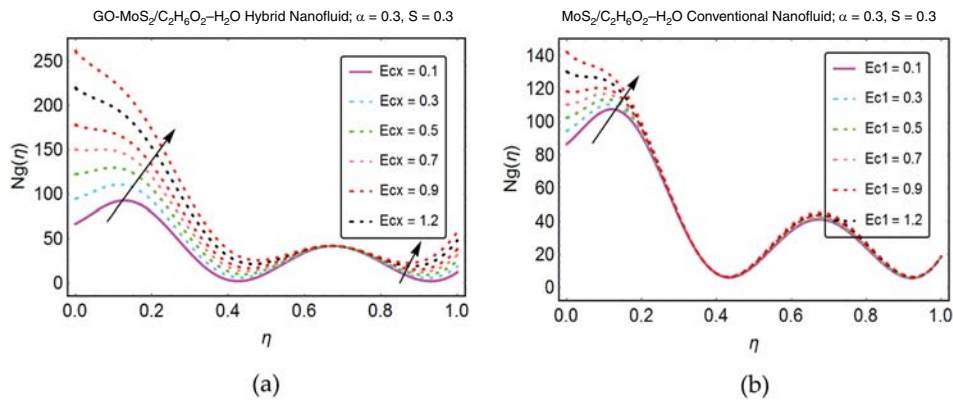


Figure 9: Influence of Ec_x on entropy generation for (a) hybrid nanofluid (b) conventional nanofluid

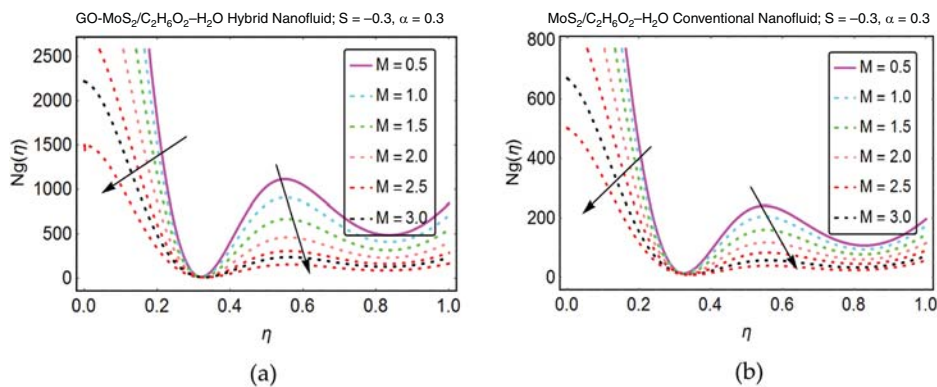


Figure 10: Influence of M , $S < 0$ on entropy generation for (a) hybrid nanofluid (b) conventional nanofluid

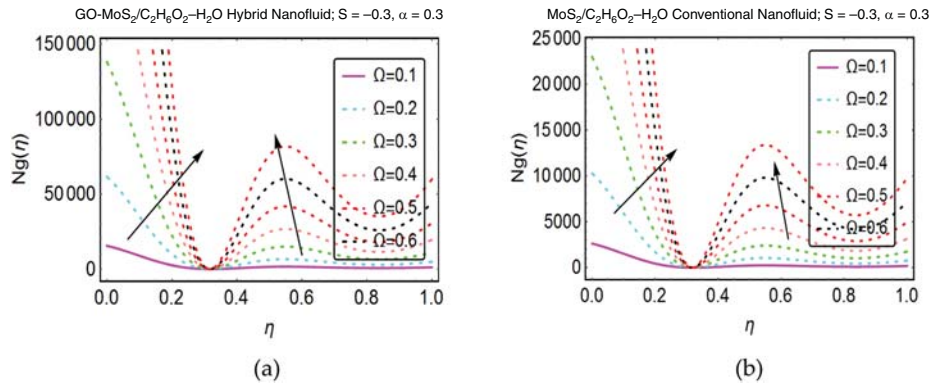


Figure 11: Influence of Ω , $S < 0$ on entropy generation for (a) hybrid nanofluid (b) conventional nanofluid

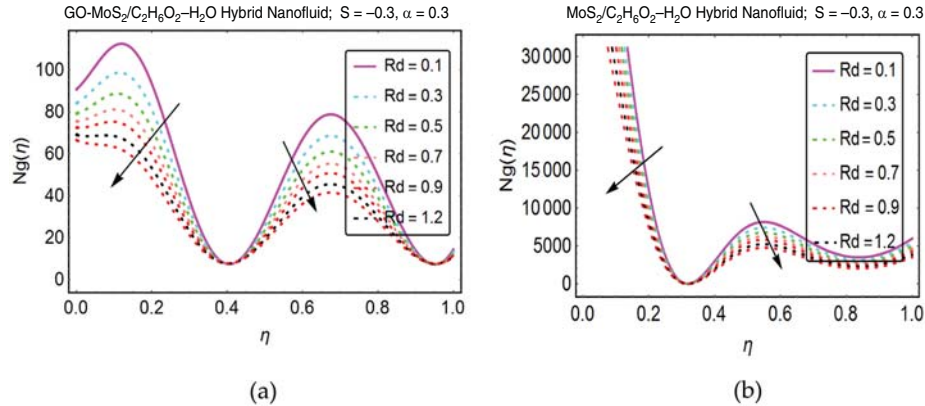


Figure 12: Influence of Rd , $S < 0$ on entropy generation for (a) hybrid nanofluid and (b) conventional nanofluid

The behavior of entropy generation is detected for both under consideration hybrid and conventional nanofluids. It is pointed that the viscous dissipation allows the rise in entropy production because due to this, internal energy of the fluid enhances due to which the entropy increases. Moreover, it is examined that the entropy drops quickly when the upper plate moves towards the lower plate and slow decrement is perceived for away movement of the upper plate.

It is analysed that the effective thermal conductivity of the hybrid nanofluid (GO-MoS₂/C₂H₆O₂-H₂O) showed dominating behaviour for varying volume fraction factor φ . Due to superior effective characteristics of the hybrid nanofluid (GO-MoS₂/C₂H₆O₂-H₂O) than conventional nanofluid (MoS₂/C₂H₆O₂-H₂O) therefore, the hybrid nanofluids are reliable for industrial and technological purposes.

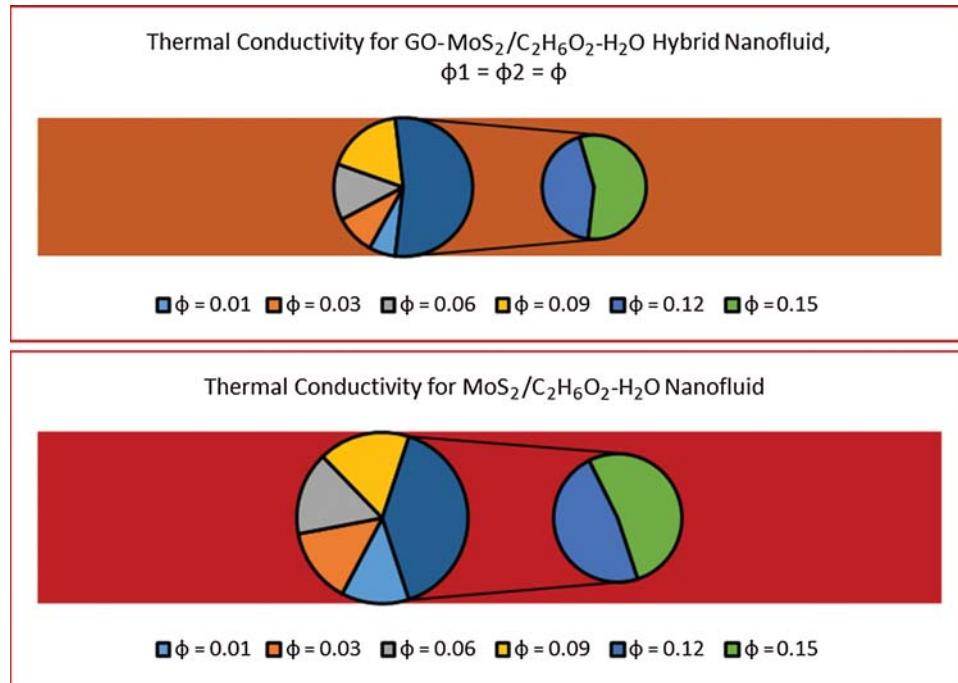


Figure 13: Influence of volume fraction on thermal conductivity for hybrid nanofluid and conventional nanofluid

5 Conclusions

The colloidal flow of GO-MoS₂/C₂H₆O₂-H₂O and MoS₂/C₂H₆O₂-H₂O is presented between parallel rotating magneto radiative plates. From the temperature and entropy analysis, it is investigated that the temperature of the hybrid and conventional nanofluids rises against the stronger thermal radiations. However, significant changes are perceived in the hybrid nanofluid. The temperature drops due to rotating plates in both fluids. The entropy generation increases for more dissipation effects and drops against the imposed magnetic effects. Further, prompt increment in thermal conductivities of the nanofluids is observed. It is also perceived that the hybrid nanofluid has high thermal performance, therefore, these fluids are reliable for the industrial and engineering uses.

Funding Statement: The author(s) received no specific funding for this study.

Conflict of Interest: The authors declare that they have no conflicts of interest to report regarding the present study.

References

- [1] N. Ahmed F. Saba, U. Khan, I. Khan, T. A. Alkanhal *et al.*, "Spherical shaped (Ag-Fe₃O₄/H₂O) hybrid nanofluid flow squeezed between two Riga plates with nonlinear thermal radiation and chemical reaction effects," *Energies*, vol. 12, 2019. <https://doi.org/10.3390/en12010076>.
- [2] S. Das, R. N. Jana and O. D. Makinde, "MHD flow of Cu-Al₂O₃/water hybrid nanofluid in porous channel: Analysis of entropy generation," *Defect Diffusion Forum*, vol. 377, pp. 42-61, 2017.

- [3] M. Mehrali, E. Sadeghinezhad, A. R. Akhiani, S. T. Latibari, C. H. S. Metselaar *et al.*, “Heat transfer and entropy generation analysis of hybrid graphene/Fe₃O₄ ferro-nanofluid flow under the influence of a magnetic field,” *Powder Technology*, vol. 308, pp. 149–157, 2017.
- [4] G. Huminic and A. Huminic, “The heat transfer performances and entropy generation analysis of hybrid nanofluids in a flattened tube,” *International Journal of Heat and Mass Transfer*, vol. 119, pp. 813–827, 2018.
- [5] S. Hussain, S. E. Ahmed and T. Akbar, “Entropy generation analysis in MHD mixed convection of hybrid nanofluid in an open cavity with a horizontal channel containing an adiabatic obstacle,” *International Journal of Heat and Mass Transfer*, vol. 114, pp. 1054–1066, 2017.
- [6] S. Ghadikolaei, K. Hosseinzadeh and D. D. Ganji, “Investigation on three-dimensional squeezing flow of mixture base fluid (ethylene glycol-water) suspended by hybrid nanoparticle (Fe₃O₄-Ag) dependent on shape factor,” *Journal of Molecular Liquids*, vol. 262, pp. 376–388, 2018.
- [7] A. Moghadassi, E. Ghomi and F. Parvzian, “A numerical study of water based Al₂O₃ and Al₂O₃-Cu hybrid nanofluid effect on forced convective heat transfer,” *International Journal of Thermal Sciences*, vol. 92, pp. 50–57, 2015.
- [8] N. Ahmed, Adnan, U. Khan and S. T. Mohyud-Din, “Unsteady radiative flow of chemically reacting fluid over a convectively heated stretchable surface with cross-diffusion gradients,” *International Journal of Thermal Sciences*, vol. 121, pp. 182–191, 2017.
- [9] N. Ahmed, Adnan, U. Khan and S. T. Mohyud-Din, “Influence of an effective Prandtl number model on squeezed flow of γ Al₂O₃-H₂O and γ Al₂O₃-C₂H₆O₂ nanofluids,” *Journal of Molecular Liquids*, vol. 238, pp. 447–454, 2017.
- [10] N. Ahmed, Adnan, U. Khan, and S. T. Mohyud-Din, “3D squeezed flow of γ Al₂O₃-H₂O and γ Al₂O₃-C₂H₆O₂ Nanofluids: A numerical study,” *International Journal of Hydrogen Energy*, vol. 42, no. 39, pp. 24620–24633, 2017.
- [11] M. M. Rashidi, N. V. Ganesh, A. K. A. Hakeem, B. Ganga and G. Lorenzini, “Influences of an effective Prandtl number model on nano boundary layer flow of γ Al₂O₃-H₂O and γ Al₂O₃-C₂H₆O₂ over a vertical stretching sheet,” *International Journal of Heat and Mass Transfer*, vol. 98, pp. 616–623, 2016.
- [12] M. Sheikholeslami, “Numerical investigation of MHD nanofluid free convective heat transfer in a porous tilted enclosure,” *Engineering Computations*, vol. 34, pp. 1939–1955, 2017.
- [13] U. Khan, N. Ahmed and S. T. Mohyud-Din, “Numerical investigation for three-dimensional squeezing flow of nanofluid in a rotating channel with lower stretching wall suspended by carbon nanotubes,” *Applied Thermal Engineering*, vol. 113, pp. 1107–1117, 2017.
- [14] S. S. Ghadikolaei and M. Gholinia, “3D mixed convection MHD flow of GO-MoS₂ hybrid nanoparticles in H₂O-(CH₂OH)₂ hybrid base fluid under effect of H₂ bond,” *International Communications in Heat and Mass Transfer*, vol. 110, pp. 104371, 2020.
- [15] A. S. Butt and A. Ali, “Analysis of entropy generation effects in unsteady squeezing flow in a rotating channel with lower stretching permeable wall,” *Journal of the Taiwan Institute of Chemical Engineers*, vol. 48, pp. 8–17, 2015.